J Mater Sci: Mater Med (2011) 22:907–915
DOI 10.1007/s10856-011-4254-2

Influence of thermal treatment on the "in vitro" bioactivity of wollastonite materials

Miguel A. de la Casa-Lillo · Pablo Velásquez · Piedad N. De Aza

Received: 24 November 2009 / Accepted: 6 February 2011 / Published online: 19 February 2011

Abstract The aim of this work was to study the influence of the composition and thermal treatment of the in vitro bioactivity of wollastonite materials obtained by sol–gel method. For this purpose, gels in the system SiO_2–CaO were obtained applying calcium nitrate and tetraethoxysilicate as precursors. The gels were heated to 700°C and then sintered up to 1400°C. The bioactivity of the gel-derived materials in simulated body fluid (SBF) was investigated and characterized. Additional changes in ionic concentration, using inductively couple plasma atomic emission spectroscopy (ICP-AES), were determined. The results showed that all materials obtained were bioactive and indicate that the absence of phosphorous in the material composition is not an essential requirement for the development of a Hydroxyapatite layer. The bioactivity was influenced by the thermal treatment, the different phases (glass-phase, wollastonite and pseudowollastonite) as well as the porous size. On the gel-derived materials the bioactivity decreased with the sintering temperature.

1 Introduction

Bioactive materials are known to bond to living bone in the body via formation of an apatite layer on their surfaces [1–8]. Because of this unusual property, they are widely studied for biomedical applications in areas including orthopedics and dentistry [9–12]. The bone-bonding mechanism is still not fully understood. However, all bioactive materials form on their surface a calcium phosphate layer that crystallizes to hydroxyapatite (HA)-like when in contact with physiological fluids [13–21]. Thus, the formation of a biologically active HA-like layer on the materials surface was proposed as the prerequisite for bonding to the living tissues [22–26]. The HA-like layer is also formed in vitro when bioactive materials are soaked in buffer solution (Tris-(hydroxymethyl) aminomethane and hydrochloric acid (SBF) at pH 7.4 [16–32]). It can be also reproduced in an acellular SBF with ion concentrations early equal to those of the human blood plasma [33]. Some SBF solutions are recently revised [34–36] and some cell culture media [37, 38] are also used. The ability to form an HA-like layer in vitro is related to bone-bonding ability or the ability to induce bone formation in vivo. Thus, in vitro studies predict the behaviour of a material inside the human body.

Since Hench and co-workers developed the first bioactive glass [39], several types of silicate glasses, glass–ceramics and calcium silicates [4–6] have been studied as biomaterials for repair and replacement of hard tissues. The results have shown that materials containing CaO and SiO_2 are bioactive, and were found to bond to living bone [40, 41]. However, most melt-derived glasses and glass–ceramics contain other elements, in more complex compositions [42, 43]. The use of the sol–gel technique allowed to obtain glasses with a simple composition which, in addition, resulted markedly more bioactive than melt-derived glasses with the same composition [44–46]. In recent years studies have appeared suggesting the possibility of applying the sol–gel method for this purpose [44–46]. The sol–gel process allows obtaining materials of higher purity, surface area and homogeneity than the fusion method. An additional advantage of this method is that glasses can be prepared at low temperatures without the need to include components

M. A. de la Casa-Lillo (✉) · P. Velásquez · P. N. De Aza
Departamento de Ciencia de los Materiales, Optica y Tecnología Electrónica, Instituto de Bioingeniería, Universidad Miguel Hernández, Edificio Vinalopó, Avda. de la Universidad s/n, 03203 Elche, Alicante, Spain
e-mail: mcasa@umh.es

aimed to decrease the melting temperature (i.e., Na_2O), which allows simplifying the composition. The purpose of the present paper was the preparation of bioactive gel-derived materials with the simplest composition 50 wt% SiO_2 and 50 wt% CaO by means of the Pereira el al. [44, 45] sol–gel method, as well as the study of the influence on the bioactivity of the initial gel composition and the crystalline phases induced by thermal treatment. The bioactivity of these materials was studied by soaking them in simulated body fluid (SBF) in order to evaluate the influence of the changes in the microstructure and the crystallization of different phases on the bioactivity of the materials as a result of different thermal treatments.

2 Materials and methods

2.1 Gel-derived materials

The gel-derived materials were synthesized by hydrolysis and polycondensation of tetraethyl orthosilicate (TEOS) and hydrated calcium nitrate in 2 N nitric acid in water. The nitric acid was used to catalyse the TEOS hydrolysis, using a molar ratio of H_2O/TEOS of 8. After the addition of each reactant, the solution was stirred for 1 h. The sol was obtained in a sealed container that was kept at room temperature to allow the hydrolysis and polycondensation reactions, until the gel was formed. Aging was performed at 70°C for 3 days in the same container. The drying of the gel was carried out by replacing the previous top by one displaying a hole with a diameter of 1 mm, to allow the leak of gases, and heating the gel at 150°C for 2 days. The dried gel was milled and sieved.

Thermogravimetric and differential thermal analysis (TG/DTA) of the dried gel were performed at a heating rate of 10°C/min, starting at room temperature up to 1350°C. The test was carried out in a platinum crucible and under atmospheric conditions. DTA results established the temperatures at which the crystalline phases formed and their possible polymorphic transformations. Based on the DTA results, the pellets were heated at 800, 900, 1000, 1200, 1300 and 1400°C at a rate of 5°C/min with a dwell of 6 h. From this temperature the samples were further cooled inside the furnace down to room temperature. These samples were compared with the material heated at 700°C, the stabilization temperature generally used for sol–gel material [44–48].

2.2 SBF in vitro test

The in vitro bioactivity study was performed by soaking the pieces in the simulated body fluid (SBF No. 9) proposed by Kokubo et al. [21] with an ion concentration nearly equal to that of human blood plasma. After being ultrasonically washed in acetone and rinsed in deionised water the pellets were soaked in 100 ml of SBF in polyethylene bottles at 36.5°C. The immersion period of the pellets in SBF was up to 4 weeks. The choice of this time span was based on the results obtained from previous in vitro experiments performed in the same media [27–32].

2.3 Sample characterization

Samples were characterized before and after the SBF in vitro test. Samples obtained after the thermal treatments were studied by X-ray Diffraction (XRD) using a Bruker D8 Advance instrument. XRD were recorded automated diffractometer using Cu $K\alpha_{1,2}$ radiation (1.5418 Å). Data were collected in the Bragg–Brentano ($\theta/2\theta$) vertical geometry (flat reflection mode) between 20 and 60° (2θ) in 0.05° steps, counting for 3 s per step. The diffractometer optic was a system of primary Soller foils between the X-ray tube and the fixed aperture slit of 1 mm. One scattered radiation slit of 1 mm was placed behind the sample, followed by a system of secondary Soller slits and the detector slit of 0.1 mm. The X-ray tube was operated at 40 kV at 30 mA.

The microstructure of the samples was studied by Scanning Electron Microscopy (SEM) using a Hitachi S-3500N, fitted with X-ray Energy-Dispersive Spectrometry (EDX). The samples surfaces, before and after the exposure to the SBF, were examined at 15 keV. The cross-sections were previously polished using diamond paste of 1 μm, cleaned in an ultrasonic bath, and carbon coated for SEM examination and microanalysis. EDX elemental maps of the cross-sections was collected for Ca, Si and P. Additional changes in ionic concentration of the SBF using Inductively Couple Plasma Atomic Emission Spectroscopy (ICP-AES) were determined.

2.4 Textural properties

After drying the samples in order to avoid the humidity, all samples were degassed at 250°C during 24 h to remove physically adsorbed molecules from their surfaces. The specific surface areas were estimated in relation to the masses of the degassed samples.

The porous texture characterisation of all the samples was carried out by physical adsorption–desorption isotherms of nitrogen at 77 K using an automatic volumetric adsorption system Autosorb-6 supplied by Quantachrome. The pore size distribution in the mesoporosity range was estimated by analysis of the adsorption and desorption curves using the BJH method [49] and assuming cylindrical pores.

3 Results

The TG/DTA results of the dried gel at 150°C for 2 days is shown in Fig. 1. The DTA show an endothermic effect around 140°C, which was attributed to the elimination of humidity from the atmosphere and the residual alcohol in the pores of the gel, corresponding to a weight loss of 14%. The endothermic peaks at 570 and 560°C, with a weight loss of 54% were attributed to the elimination of the nitrates introduced as calcium nitrate in the preparation of sol. These results agree with those of Duval [50], which indicated that calcium nitrate is stable up to 475°C and from that temperature the NO_2 elimination starts. Then the weight remains almost constant up to 1350°C. The exothermic maximum at 900°C is due the crystallization of the wollastonite-2M. This finding was confirmed by XRD analysis of the quenched sample from 1000°C. The small endothermic effect at ~1200°C was due to the polymorphic transformation of wollastonite-2M into pseudowollastonite also confirmed in the XRD analysis of the residue TG/DTA.

Figure 2 shows the XRD patterns of the pellets heated at different temperatures. The materials treated at 700 and 800°C showed XRD patterns typical of amorphous materials and no crystalline phases were detected. Glass crystallization was observed from 900°C. The samples heated between 900 and 1200°C show peaks that correspond to wollastonite-2M (low temperature form of wollastonite) and at 1200°C the crystallization of pseudowollastonite starts, presenting the XRD a mixture of wollasotnite-2M and pseudowollastonite. However, in the sample heated at 1300°C the wollastonite-2M phase was transformed into pseudowollastonite, which is the most stable phase at high temperature. At higher temperature (1400°C) the pseudowollastonite is the only phase present.

Figure 3 shows the nitrogen adsorption isotherms at 77 K (Fig. 3a) of the samples and the pore size distribution (Fig. 3b) for those two samples without heat treatment after the stabilization of the sol–gel material. The isotherms of these samples are type IV and show the typical hysteresis of mesoporous materials [51]. In the samples heat treated at temperatures above 800°C the volume of mesopores is almost negligible.

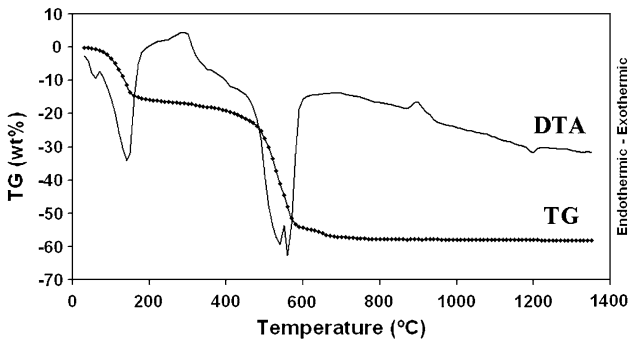

Fig. 1 DTA and TG curves of the gel powder after being dried at 150°C

The bioactivity study was made in samples treated at 1000, 1200 and 1400°C, because these samples are representative of the different phase composition and microstructures of the obtained glass–ceramics. The behaviour of these samples was compared with that of material treated at 700°C. The SEM micrographs of samples surface after polishing and chemical etching with diluted acetic acid during 5 s are shown in Fig. 4. The micrographs show a microstructure formed by irregular particles of different size with a homogeneous distribution. The temperature promotes an increase in the number and in the size of the particles, and in addition, the glassy phase diminishes. Figure 4a shows a typical homogeneous glass without microstructure on it. EDX analysis of the particles confirm the presence of CaO and SiO_2 in the grains with a 1:1 molar ratio, the same as the theoretical composition of $CaSiO_3$. The EDX analysis of the silica-rich glassy phases present a molar SiO_2/CaO ratio of 0.73. The sintering process took place in the sample of 1400°C where the amount of glassy phase is very small (Fig. 4d).

After 1 week soaking in SBF it was observed that a new layer covered homogeneously the surface of all materials (Fig. 5). The layer morphology and the formation rate of this layer depended on the thermal treatment. The fastest formation of the layer (5 h) was observed in samples treated at 700°C. This layer was composed by spherical particles smaller than 0.6 μm in diameter, some of which reach the size of 1.5 μm after 1 week of soaking. This morphology does no further change with soaking time (from 1 to 4 weeks) although the density of the layer increases. In samples treated at higher temperatures the layer appeared after longer soaking times but once this layer was formed, the spherical particles could be appreciated. In sample 1000°C the layer was observed after 3 days, whereas in the samples heated at 1200 and 1400°C the layer was not observed until after 5 days.

Table 1 shows the results of the EDX analysis of samples surface after 7 days of soaking in SBF. The results after immersion in SBF showed that the Si content decreased significantly while the Ca and P content increased, indicating that the layer formed on the samples surface is rich in calcium and phosphorus. The EDX analysis of the surface without spherical precipitated of sample 1200 and 1400°C showed a higher content of Si and lower content of Ca that of the surface before soaking in SBF. This effect indicates a higher solubility of $CaSiO_3$-phase and therefore SiO_2-rich surface obtained.

Figure 6 shows the microstructure of the cross-section of 700°C gel derived material after 28 days in SBF. The

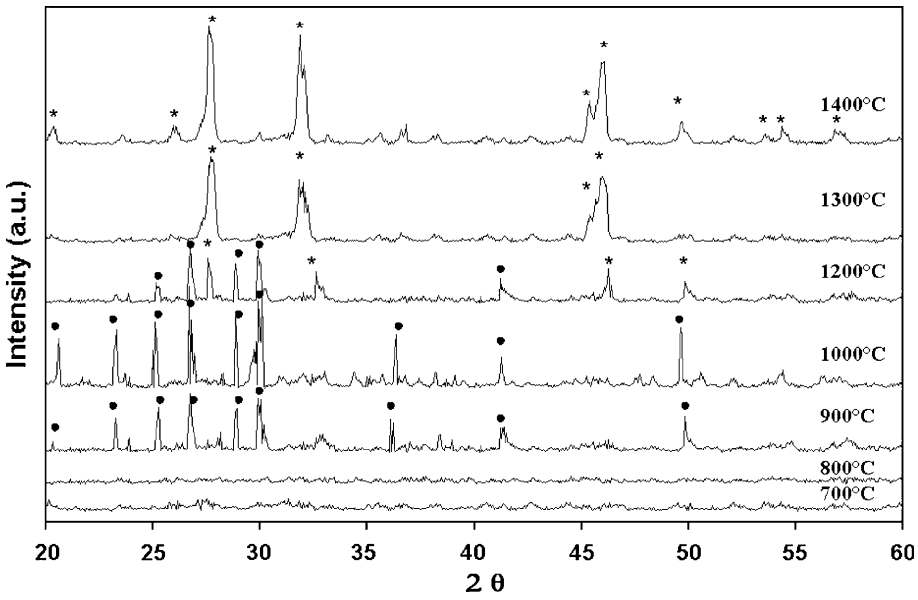

Fig. 2 XRD patterns of samples treated at different temperatures (*filled circle* wollastonite-2M, *asterisks* pseudowollastonite

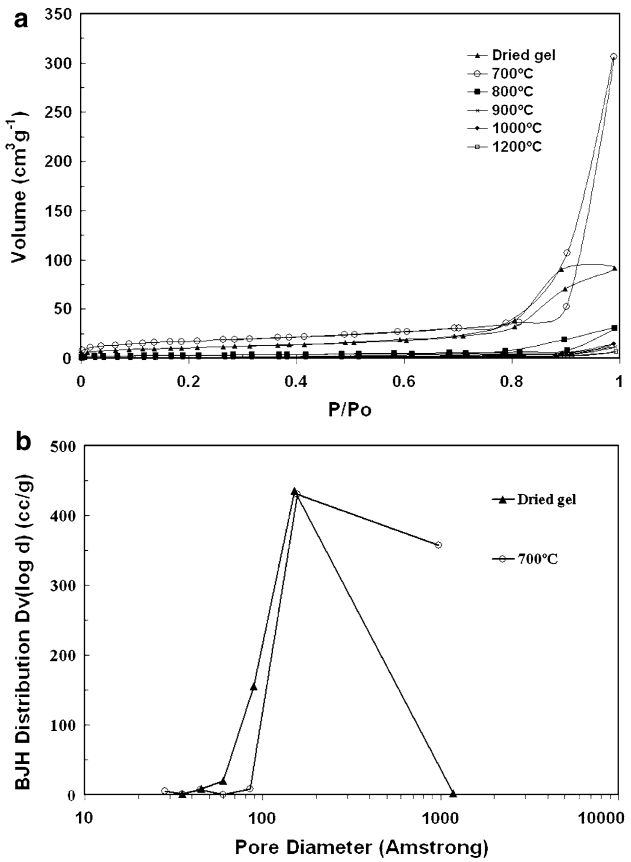

Fig. 3 **a** N_2 isotherms at 77 K, **b** BJH pore size distribution

elemental X-ray maps of silicon, calcium and phosphorus are also presented. The outer layer, with an average thickness of about 45 μm (±1 μm), was composed of a Ca/P-rich phase, while the underlayer in direct contact with the material substrate was rich in silicon. The crack visible in the figure between the specimen surface and Ca/P-layer is an artifact caused by the polishing of the specimen.

Changes in the elemental ionic concentrations of SBF after 28 days of immersion are shown in Fig. 7. The chemical analysis of the SBF used in the study agreed with the composition of the one reported in the literature [21]. It was found that calcium and silicon ion concentrations in SBF increased slightly over the exposure time indicating partial dissolution of the gel derived material. On the other hand, phosphorous ion concentration decreased more significantly because of the precipitation of Ca–P phase on the surfaces of the gel derived materials. Although the formation of Ca–P phase consumed some calcium ions, the calcium ions dissolution from the gel derived material were more than those consumed. This results in a porous Ca/P layer structure that provides a path for the dissolution of both the underlying $CaSiO_3$ grains and the amorphous SiO_2 interlayer. However, the dissolution of the $CaSiO_3$ grains is suppressed gradually when the Ca/P layer reaches an appropriate thickness. Thus the Ca and Si concentrations in the SBF solution approach an apparent equilibrium state after prolonged soaking (14 days) of the gel-derived $CaSiO_3$ materials.

Figure 8 shows the change of thickness of the Ca/P layer as a function of soaking time. In the 1000°C glass–ceramic, a significant thickness of Ca/P layer forms at a rate of about 4.8 μm per day after 7 days of soaking. The formation rate gradually slows down after prolonged soaking due to the depletion of P from the SBF solution (~0.5.7 μm per day) reaching a total thickness of ~44.4 μm after 28 days. In the 1400°C glass–ceramic, the Ca/P layer reached a thickness of about ~35 μm after 28 days of soaking,

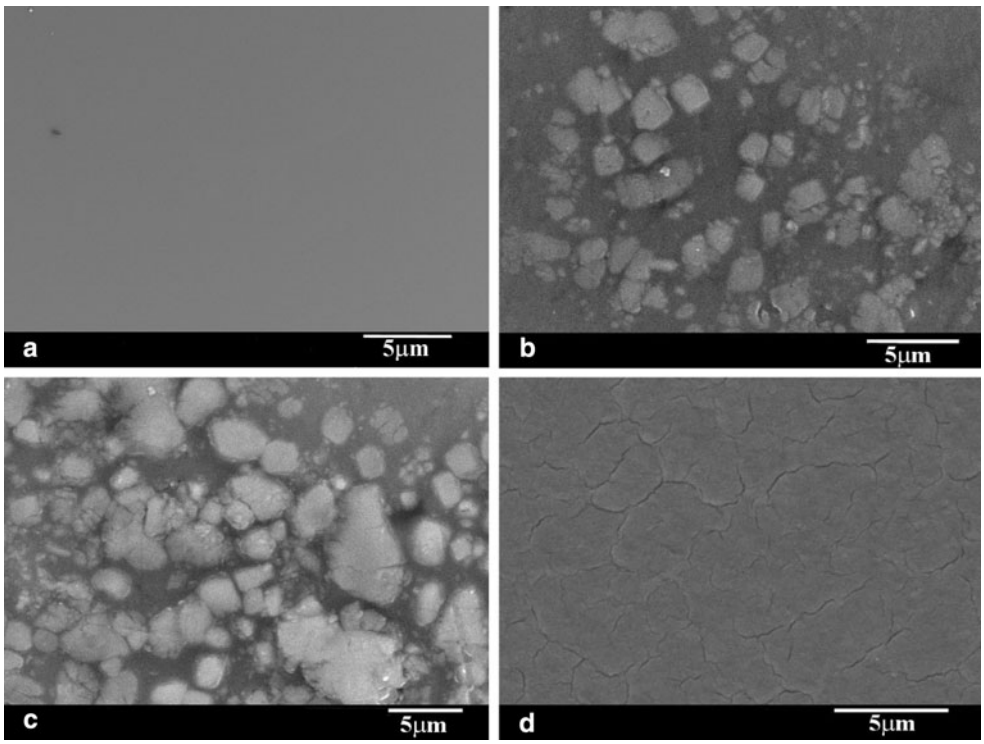

Fig. 4 SEM images of the microstructure of the gel-derived materials at **a** 700, **b** 1000, **c** 1200 and **d** 1400°C

corresponding to the formation of Ca/P layer with ball-like particle morphology attached to the 1400°C glass–ceramic surfaces. The formation rate and thickness of Ca/P layer formed on the glass–ceramic were much greater than various reference materials, such as A-W glass–ceramic, as reported by Kokubo [52] and Liu [53], respectively. The good bioactivity of the present gel derived $CaSiO_3$ materials is considered to be due to the influence of their solubility in SBF solution and to the presence of the silica rich glassy phase, which induces rapid nucleation and growth of the Ca/P layer in the surface.

4 Discussion

Since $CaSiO_3$ grains are reported to dissolve more slowly in SBF solution than the silica-rich glassy phase at the grain boundaries [13, 23, 27, 28, 47], the differences in microstructure between the 700 and the 1000, 1200 and 1400°C glass–ceramic materials are considered to influence the formation of Ca/P layer on their surfaces. The 1000°C glass–ceramic material consists of small wollastonite-2M grains and silica-rich glassy phase, which is suggested to promote surface dissolution with the formation of silanol at the surface of the amorphous SiO_2 interlayer. These processes should proceed prior to the formation of the Ca/P layer, increasing the Ca and Si concentrations in the SBF solution (Fig. 6) in contact with the 1000°C glass–ceramic to suitable levels for rapid Ca/P layer formation. On the other hand, the very small amount of glassy phase at the grain boundaries for the 1400°C glass–ceramic materials can be considered the cause for the slow formation rate of the amorphous SiO_2 interlayer and the slower dissolution rate of the pseudowollastonite grains. This means that the Ca/P layer appears later in this sample (7 days) than in the samples with a high content of silica-rich glassy phase (3 days).

Our gel-derived materials abruptly decreased the volume of mesopores when they were heat-treated at temperatures above 800°C, as shown in Fig. 3. The heat treatment causes the disappearance of the porosity. This indicates that the numbers of active sites for apatite nucleation on the surface of the gel-derived materials were abruptly reduced by heat treatment above 800°C. Therefore the rate of apatite nucleation on the gel-derived materials was controlled not only by the catalytic effect of the surface of the gel-derived materials, but also by ion dissolution from the gel-derived materials.

Generally, the rate of apatite formation in an aqueous solution is controlled by nucleation and crystal growth. These are possible only within a supersaturated environment. As it is well known, the body fluid is already supersaturated with respect to the apatite even under normal condition [54]. In such an environment, once apatite nuclei are formed, they can grow spontaneously by consuming calcium and phosphate ions from the surrounding

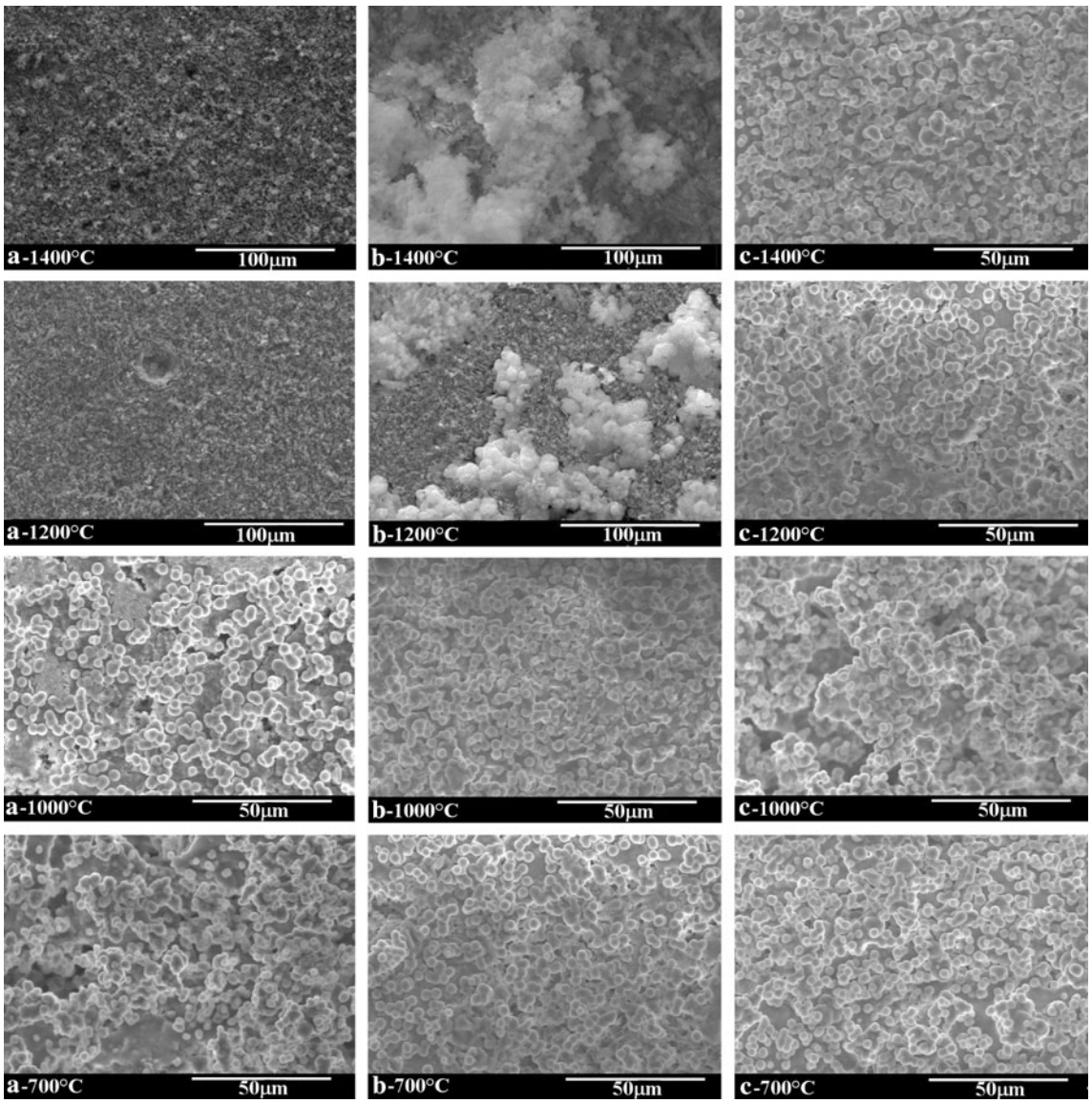

Fig. 5 SEM images of the samples after immersion in SBF for **a** 3, **b** 7 and **c** 28 days

fluid. The rate of formation of apatite in a body environment is, therefore, determined by the rate of apatite nucleation. In view of this, it can be seen from the present results that the rate of apatite nucleation decreases remarkably by the heat treatment of gel derived materials above 700°C.

This observation confirms also the results obtained by other authors [42, 43, 47]. Hench et al. reported also previously that the apatite-forming ability of a gel was lost when the gel was heat-treated at 900°C [55]. In their case, however, the gel contained CaO and P_2O_5, beside the SiO_2, while the test solution contained neither calcium nor phosphate ions. Also, Padilla et al. [56] in a gel containing $CaO–SiO_2–P_2O_5$ reported that the sintering process plays an important role in the bioactivity of the heated materials, indicating that the apatite formation rate decreases with the sintering temperature and the content of pseudowollastonite phase in the materials.

5 Conclusions

All the gel-derived $CaSiO_3$ materials studied are bioactive, growing an apatite layer on their surface, by taking phosphorous from the SBF.

The sintering process played an important role in the bioactivity of heated samples, where the glassy phase, Wollastonite-2M and pseudowollastonite phase were the

Table 1 Surface composition (at%) obtained by EDX of samples before and after 7 days soaking in SBF

	Si	Ca	P
Before soaking	49	51	–
7 days soaking			
700°C	3	69	28
1000°C	2	75	23
1200°C layer	1	62	37
1200°C surface	87	12	1
1400°C layer	1	65	34
1400°C surface	90	10	–

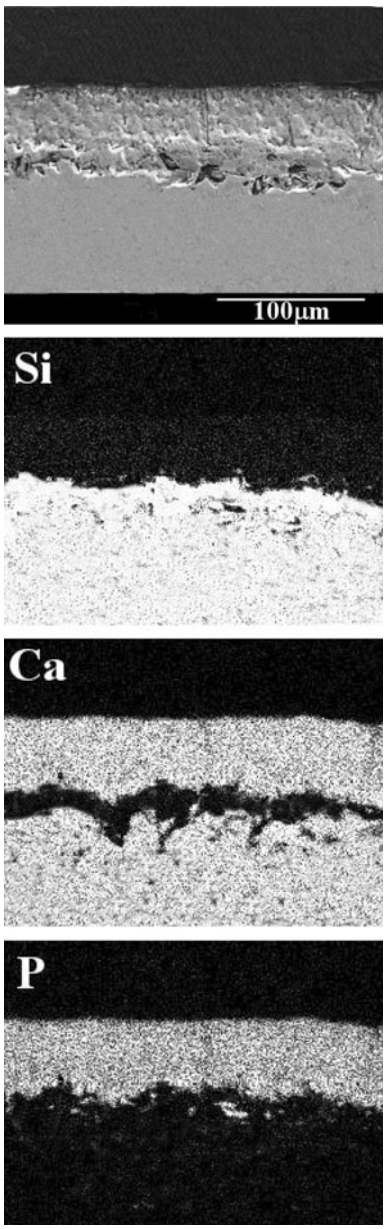

Fig. 6 X-ray elemental maps of Si, Ca, P, and a relevant SEM image of the cross-section of the 700°C glass after 4 week of immersion in SBF

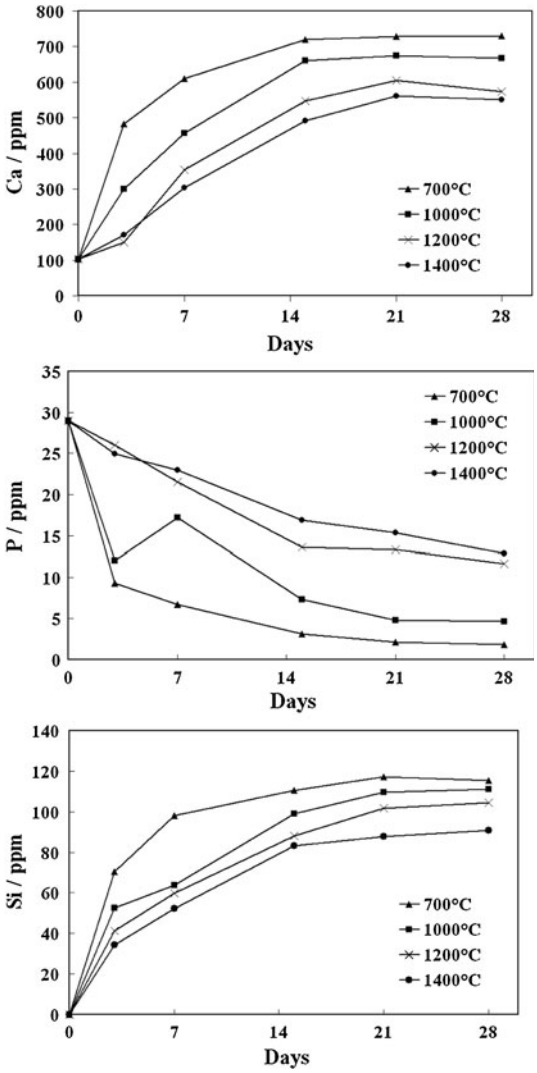

Fig. 7 Changes of Ca, P and Si concentration of the SBF solution measured by ICP after soaking the gel-derived materials for various periods

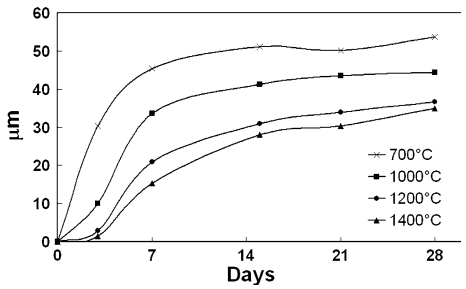

Fig. 8 Change of thickness of the Ca–P layer of the gel-derived materials as a function of soaking time

main phases. It was observed by the ionic changes in the SBF that the layer formation rate decreased with the sintering temperature. In these samples, the sintering process seems to hinder the dissolution process of wollastonite,

mainly from the bulk, and therefore delays the formation of the apatite layer.

Acknowledgment Part of this work was supported by CICYT under project no. MAT2006-12749-C02-02.

References

1. Hench LL, Wilson JW. Surface-active biomaterials. Science. 1984;226:630–6.
2. Gross U, Kinne R, Schmitz HJ, Strunz V. The response of bone to surface active glass/glass-ceramics. CRC Crit Rev Biocompat. 1988;4:2–16.
3. Bonfield W, Luklinska ZB. High-resolution electron microscopy of a bone implant interface. In: Davis JE, editor. The bone-biomaterial interface. Toronto: University of Toronto Press; 1991. p. 89–93.
4. Ohura K, Nakamura T, Yamamuro T, Kokubo T, Ebisawa T, Kotoura Y, Oka M. Bone-bonding ability of P_2O_5-free CaO SiO_2 glasses. J Biomed Mater Res. 1991;25:357–65.
5. Cao W, Hench LL. Bioactive materials. Ceram Int. 1996;22:493–507.
6. Clèries L, Fernández-Pradas JM, Morenza JL. Bone growth on and resorption of calcium phosphate coatings obtained by pulsed laser deposition. J Biomed Mater Res. 2000;49:43–52.
7. De Aza PN, De Aza AH, De Aza S. Crystalline bioceramic materials. Bol Soc Esp Ceram Vidrio. 2005;44(3):135–45.
8. De Aza PN, De Aza AH, Pena P, De Aza S. Bioactive glasses and glass-ceramics. Bol Soc Esp Ceram Vidrio. 2007;46(2):45–55.
9. Van Blitterswijk CA, Hesseling SC, Grote JJ, Koerten HK, de Groot K. The biocompatibility of hydroxyapatite ceramic: a study of retrieved human middle ear implants. J Biomed Mater Res. 1990;24:433–53.
10. Buser D, Dula K, Beser U, Hirt HP, Berthold H. Localised ridge augmentation using guide bone regeneration. I. Surgical procedure in the maxilla. Int J Periodontics Restor Dent. 1993;13:29–45.
11. Yamamuro Y. A-W glass-ceramic: clinical applications. In: Hench LL, Wilson J, editors. An introduction to bioceramics. Singapore: World Scientific Publishing Co.; 1993. p. 89.
12. Negroiu G, Piticescu RM, Chitanu GC, Mihailescu IN, Zdrentu L, Miroiu M. Biocompatibility evaluation of a novel hydroxyapatite-polymer coating for medical implants (in vitro tests). J Mater Sci Mater Med. 2008;19:1537–44.
13. Ohtsuki C, Kokubo T, Yamamuro T. Mechanism of apatite formation on CaO-SiO_2-P_2O_5 glasses in a simulated body fluid. J Non-Cryst Solids. 1992;143:84–92.
14. Nonami T. In vivo and in vitro testing of diopside for biomaterials. J Soc Mater Eng Resour Jpn. 1995;8(2):12–8.
15. De Aza PN, Luklinska ZB, Anseau M, Guitian F, De Aza S. Bioactivity of pseudowollastonite in human saliva. J Dent. 1999;27:107–13.
16. Dorozhkin SV, Schmitt M, Bouler JM, Daculsi G. Chemical transformation of some biologically relevant calcium phosphates in aqueous media during a steam sterilization. J Mater Sci Mater Med. 2000;11:779–86.
17. De Aza PN, Luklinska Z, Anseau M, Hector M, Guitian F, De Aza S. Reactivity of a wollastonite-tricalcium phosphate bioeutectic in human parotid saliva. Biomaterials. 2000;21(17):1735–41.
18. De Aza PN, De Aza S. Bioactivities of a SiO_2-CaO-ZrO_2 in simulated body fluid and human parotid saliva. Key Eng Mater. 2004;254–256:75–8.
19. De Aza PN, Luklinska Z, Anseau M. Bioactivity of diopside ceramic in human parotid saliva. J Biomed Mater Res. 2005; 73B(1):54–60.
20. Ohsawa K, Neo M, Okamoto T, Tamura K, Nakamura T. In vivo absorption of porous apatite and wollastonite containing glass ceramic. J Mater Sci Mater Med. 2004;15:859–64.
21. Kokubo T, Kushitani H, Sakka S, Kitsugi T, Yamamuro T. Solutions able to reproduce in vivo surface-structure changes in bioactive glass-ceramics A-W. J Biomed Mater Res. 1990;24: 721–34.
22. Kamitakahara M, Yagi T, Ohtsuki C. Effect of preparation conditions on the properties of bioactive glasses for testing SBF. J Mater Sci Mater Med. 2009;20(12):2419–26.
23. Ohtsuki C, Aoki Y, Kokubo T, Bando Y, Neo M, Yamamuro T, Yacamura T. Characterization of apatite layer formed on bioactive glass-ceramic A-W. Bioceramics. 1992;5:87–94.
24. De Aza PN, Luklinska ZB, Martínez A, Anseau MR, Guitian F, De Aza S. Morphological and structural study of pseudowollastonite implants in bone. J Microsc (Oxf). 2000;197:60–7.
25. De Aza PN, Luklinska ZB, Anseau MR, Guitian F, De Aza S. Transmission electron microscopy of the interface between bone and pseudowollastonite implant. J Microsc (Oxf). 2001;201: 33–43.
26. De Aza PN, Luklinska Z, Santos C, Guitian F, De Aza S. Mechanism of bone-like apatite formation on a bioactive implant in vivo. Biomaterials. 2003;24:1437–45.
27. De Aza PN, Guitian F, De Aza S. Bioactivity of wollastonite ceramics: in vitro evaluation. Scripta Metall Mater. 1994;31: 1001–5.
28. De Aza PN, Guitian F, De Aza S. Polycrystalline wollastonite ceramics. Biomaterials free of P_2O_5. In: Vincenzini P, editor. Advances in science and technology. vol. 12. Materials in clinical application. Faenza: Techna Srl; 1995. p. 19–27.
29. De Aza PN, Luklinska Z. Efecto de la microestructura sobre la bioactividad de dos materiales vitroceramicos del sistema $CaSiO_3$-ZrO_2. Bol Soc Esp Ceram Vidrio. 2003;42(2):101–6.
30. De Aza PN, Luklinska Z. Effect of the glass-ceramic microstructure on its in vitro bioactivity. J Mater Sci Mater Med. 2003;14(10):891–8.
31. De Aza PN, Fernandez-Pradas JM, Serra P. In vitro bioactivity of laser ablation pseudowollastonite coating. Biomaterials. 2004;25: 1983–90.
32. Alemany MI, Velásquez P, de la Casa-Lillo MA, De Aza PN. Effect of materials' processing methods on the "in vitro" bioactivity of wollastonite glass-ceramic materials. J Non-Cryst Solids. 2005;351:1716–26.
33. Kokubo T, Ito S, Huang T, Hayashi T, Sakka S, Kitsugi T, Kitsugi T, Yamamuro T. Ca, P-rich layer formed on high-strength bioactive glass-ceramic A-W. J Biomed Mater Res. 1990;24: 331–43.
34. Oyane A, Kim HM, Furuya T, Kokubo T, Miyazaki T, Nakamura T. Preparation and assessment of revised simulated body fluids. J Biomed Mater Res. 2003;65A:188–95.
35. Oyane A, Onuma K, Ito A, Kim HM, Kokubo T, Nakamura T. Formation and growth of clusters in conventional and new kinds of simulated body fluids. J Biomed Mater Res. 2003;64A: 339–48.
36. Takadama H, Hashimoto M, Mizuno M, Kokubo T. Round-robin test of SBF for in vitro measurement of apatite-forming ability of synthetic materials. Phosphorus Res Bull. 2004;17:119–25.
37. Dufrane D, Delloye C, McKay I, De Aza PN, De Aza S, Shneider YJ, Anseau M. Indirect cytotoxicity evaluation of pseudowollastonite. J Mater Sci Mater Med. 2003;14(1):33–8.
38. Sarmento C, Luklinska ZB, Brown L, Anseau M, De Aza S, De Aza PN, Hughes SF, McKay IJ. The in vitro behaviour of osteoblastic cell cultured in the presence of pseudowollastonite ceramic. J Biomed Mater Res. 2004;69A(2):351–8.

39. Hench LL, Spinter RJ, Allen WC, Greenlee TK Jr. Bonding mechanisms at the interface of ceramic prosthetic materials. J Biomed Mater Res. 1971;2:117–41.
40. Kitsugi T, Nakamura T, Yamamuro T, Kokubo T, Shibuya T, Takagi M. SEM-EPMA observation of three types of apatite containing glass ceramics implanted in bone: the variance of a Ca, P-rich layer. J Biomed Mater Res. 1987;21:1255–71.
41. Ebisawa T, Kokubo T, Ohura K, Yamamuro T. Bioactivity of CaO SiO_2-based glasses: in vitro evaluation. J Mater Sci Mater Med. 1990;1(4):239–44.
42. Kokubo T, Ito S, Sakka S, Yamamuro T. Formation of a high-strength bioactive glass-ceramic in the system MgO-CaO-SiO_2-P_2O_5. J Mater Sci. 1986;21:536–40.
43. Eriksson G, Wu P, Blander M, Pelton AD. Critical evaluation and optimisation of the thermodynamic properties and phase diagrams of the MnO-SiO_2 and CaO-SiO_2 systems. Can Metall Q. 1994;33:13–21.
44. Pereira MM, Clark AE, Hench LL. Calcium-phosphate formation on sol-gel derived bioactive glasses in vitro. J Biomed Mater Res. 1994;28(6):693–8.
45. Pereira MM, Clark AE, Hench LL. Effect of texture on the rate of HA formation on gel-silica surface. J Am Ceram Soc. 1995; 78(9):2463–8.
46. Ortega-Lara W, Cortés-Hernandez DA, Best S, Brooks R, Bretado-Aragón L, Rentería-Zamarrón D. In vitro bioactivity of wollastonite-titania materials obtained by sol-gel method or solid state reaction. J Sol-Gel Sci Technol. 2008;48:362–8.
47. Izquierdo-Barba I, Vallet-Regi M. In vitro calcium phosphate layer formation on sol-gel glasses on the CaO-SiO_2 system. J Biomed Mater Res. 1999;47:243–50.
48. Laczka M, Cholewa K, Laczka-Osyczka A. Gel derived powders of CaO-P_2O_5-SiO_2 system as a starting material to production of bioactive ceramics. J Alloys Compd. 1997;248:42–51.
49. Lowell S, Shields JE. Powder surface area and porosity. London: Chapman and Hall; 1984.
50. Duval C. Inorganic thermogravimetric analysis. New York: Elsevier; 1963. p. 274.
51. Sing KSW, Everet DH, Haul RAW. Reporting physisorption data for gas/solid systems. Pure Appl Chem. 1985;57:603–19.
52. Kokubo T. Surface chemistry of bioactive glass-ceramics. J Non-Cryst Solids. 1990;120:138–51.
53. Liu DM. Bioactive glass-ceramic: formation, characterization and bioactivity. Mater Chem Phys. 1994;36:294–303.
54. Neuman W, Neuman M. The chemical dynamics of bone mineral. Chicago: University of Chicago; 1958. p. 34.
55. Li R, Clark AE, Hench LL. Effects of structure and surface area on bioactive powders by the sol-gel process. In: Hench LL, West JK, editors. Chemical processing of advanced materials. New York: Wiley; 1992. p. 627–34.
56. Padilla S, Roman J, Carenas A, Vallet-Regi M. The influence of the phosphorus content on the bioactivity of sol-gel glass ceramics. Biomaterials. 2005;26:475–83.